Available online at www.sciencedirect.com
ScienceDirect
ELSEVIER
Ceramics International 33 (2007) 1025–1031
CERAMICS INTERNATIONAL
www.elsevier.com/locate/ceramint

Dispersion and stability of 8 mol.% yttria stabilized zirconia suspensions for dip-coating filtration membranes

Yong Hong Wang, Xing Qin Liu *, Guang Yao Meng

Department of Materials Science and Engineering, University of Science & Technology of China, Hefei, Anhui 230026, PR China

Received 28 October 2005; received in revised form 22 January 2006; accepted 10 March 2006
Available online 20 October 2006

Abstract

The dispersion and the stability of the suspensions from commercially available 8 mol.% yttria stabilized zirconia (8YSZ) powder have been systematically investigated as a function of the system factors such as pH value, temperature, solid loadings, molecular weight and amounts of polyacrylic acid (PAA) dispersant. The interaction mechanisms between YSZ particles and organic additives in suspensions were analyzed and discussed in detail. The crack-free tubular membranes derived from the fully dispersed and well stabilized YSZ suspensions with appropriate viscosity exhibited an average pore diameter of 0.31 μm and membranes thickness of 10 μm. The pure water permeability of the membrane was up to 1.7 $m^3 h^{-1} bar^{-1} m^{-2}$.

Keywords: A. Suspensions; D. ZrO_2; E. Membranes; Rheology

1. Introduction

Compared with alumina ceramic membranes, zirconia ceramic membranes have been favored by ceramic experts for its excellent mechanical performance, thermal stability, resistance to caustic medium and biological attack [1]. However, membrane defects arising from phase transition during high temperature thermal treatment process often occur when the metastable tetragonal type zirconia was selected as membranes materials [2]. A feasible solution to solving this difficulty with doped ≥8 mol.% yttria stabilized zirconia (vig. Y-TZP or YSZ) as starting membranes materials have been successfully applied into the synthesis of crack-free YSZ membranes that will be further utilized as supports for ultra-thin dense YSZ and other ceramic or metallic membranes [3–7].

Crack-free YSZ membranes have been largely made by sol–gel methods [3–5]. Nevertheless, in comparison to the sol–gel routes, the dip-coating process is an easy and inexpensive method for preparation of ceramic membranes. Kim and Lin [6] have prepared defects-free supported YSZ membranes derived from stable aqueous suspensions constituted by commercial YSZ powder. Recently, in our groups, Zhang et al. [7] obtained a fully dispersed suspensions with nanosize YSZ powder and produced dense crack-free thin films by repeated dip-coating techniques. Chao et al. [8] also prepared the tubular composite ZrO_2/Al_2O_3 microfiltration membranes by applying the suspensions of zirconia particles with mean pore diameter 0.2 μm. They all claimed that they had obtained exciting results by the dip-coating techniques from a desired suspensions, however, they all excessively focused on the structure and the properties of developed membranes and the detailed investigation on the dispersion characteristics of desired 8YSZ suspensions required for dip-coating process were yet lean. Moreover, few articles on preparation of 8YSZ microfiltration membrane were reported, which are likely attributed to the difficulties in dispersing and stabilizing 8YSZ suspensions suitable for dip-coating ten micron thickness membrane with lower solid loading (≤20 wt.%), higher specific gravity and the character of Zr^{4+} prone to hydrating causing the rapid colloid particles growth rate [5]. In addition, doped-Y_2O_3 dissolved out of YSZ in low pH solution could redeposit onto the surface of YSZ particles and alternate the surface chemistry of YSZ particles [9]. Considering the influence of doped yttria on the suspension stability, some recent articles have been centering on low yttria content YSZ (e.g., 3Y–TZP) system [8,10]. As

---

* Corresponding author. Tel.: +86-551-3606249; fax: +86-551-3607627.
E-mail addresses: wangton@mail.ustc.edu.cn (Y.H. Wang), xqliu@ustc.edu.cn (X.Q. Liu).

0272-8842/$32.00 © 2006 Elsevier Ltd and Techna Group S.r.l. All rights reserved.
doi:10.1016/j.ceramint.2006.03.011

stated, the utilization of stable doped-yttria zirconia as membranes materials on one hand can avoid high temperature structure instability, but on the other hand is bogged with the difficulty of dispersion and stability.

Our work intends to prepare a stable and well dispersed suspensions suitable for easy dip-coating crack-free membranes on porous support with commercial 8YSZ fine powder. Besides, it focuses on the effects of experimental conditions on the dispersion and stability of 8YSZ suspension such as the selected dispersant PAA (polyacrylic acid), temperature, etc., in order to further understand the stabilization mechanism of YSZ–PAA suspensions. Next, we will verify the properties of the 8YSZ suspensions according to the related performances of the resulting membrane from the suspensions prepared.

2. Experimental procedures

Starting materials include commercial 8YSZ powder and polyacrylic acid (PAA) with different molecular weight. The YSZ powder with median particle size 1.05 μm as claimed by the supplier have a sinter density of 6.02 g m^{-3}, a BET surface area 8.40 m^2 g^{-1} and particle size in suspensions is characterized on the particle size analyzer (NSKC-1A, NanJing, China). Self-made 19 channels α-Al_2O_3 tubular supports with mean pore size 0.80 μm were used for dip-coating 8YSZ ceramic membranes. Both $NH_4{\cdot}H_2O$ and HNO_3 were marked with standardized analytical-grade reagent. Zeta potential values of YSZ powder with the varying pH were determined on the Zetasizer plus (3000HS/1000HS, Malvern Instruments Ltd., UK). Sample suspensions were diluted with a 1 mM NaCl solution to a low concentration of 0.01 vol.% and ultrasonicated for 30 min prior to zeta potential measurement.

The mixture containing YSZ powder, de-ionized water, PAA was ball-milled for 24 h by a certain order and predetermined proportions between each species with ZrO_2 ball as milling medium. Then, the pH value of YSZ suspensions was measured by pHS-25 model pH device (ShangHai, China) and adjusted with $NH_4{\cdot}H_2O$ or HNO_3; the apparent viscosity and rheological character of YSZ suspensions were performed on a NDJ-1 model rotational viscometer (ShangHai, China); quantitative study of PAA-adsorbed YSZ powder was conducted with DT-50 model differential thermal analyzer and TG-50 thermal gravimetric analyzer (Sahimadzu Corporation, Japan; standard reference:α-Al_2O_3 powder). The IR spectra of PAA-adsorbed YSZ powder was studied by FT-IR (EQUINOX55, Bruker) and samples were prepared with KBr plate. The apparent stability of YSZ suspension was characterized by sedimentation methods. After settling some times, it is recorded by the relative weight percentage of sedimentation powder to total original powder (all in dry weight). The lower the sedimentation percent value, the more stable the YSZ suspension. Next, in order to obtain the YSZ membrane, the well dispersed and stable YSZ suspensions prepared above were submitted to several steps, dip-coating, drying and sintering with programmed temperature furnace according to the predetermined temperature. Finally, the dispersion of YSZ suspensions and the microstructure of YSZ membranes were observed in a X-650 model SEM (HITACHI, JAPAN), the bubble-point method was routinely employed to get membrane pore size and distribution, N_2 gas permeation and water flux through YSZ membrane tube were measured on a pilot plant working permeation device at ambient temperature.

3. Results and discussion

3.1. 8YSZ fine powder characteristics

Fig. 1 reveals that the surface potential of 8YSZ particle is little positive in de-ionic water solution. The charged mechanism occurring in various pH ranges follows Eq. (1):

$$MOH_2{}^{+}(\text{surface}) \xleftarrow{H^+} MOH(\text{surface}) \xrightarrow{OH^-} MO^{-}(\text{surface}) + H_2O \tag{1}$$

where M is metal ion, mainly in terms of ZrO_2, Y_2O_3 in this work, which is reflected in Fig. 1 YSZ particle surface potential as function of pH value. Furthermore, from Fig. 1, naked YSZ powder isoelectric point (IEP) locates at pH 6.5 or so, which is close to that of Fengqiu et al. [11] reported IEP = 5.8–6.0 in 3Y-TZP powder and deviates far from that of Shojai et al. [12] IEP = 7.6 for 3Y–ZrO_2 due to the yttria content as high as 8 mol.% in this work and the various metal oxide impurities. Yttria is highly basic and has a significant solubility below pH 7 and dissolved yttria can greatly affect the surface chemistry and IEP [9]. In addition, the concomitant existence of other metal oxide impurities with YSZ powder may also influence on the surface chemistry of YSZ particles resulting from the hydration and polarization in solution. A dramatic shift in the IEP from about 6.5 to ca. 4.2 occurred when PAA was added into the YSZ suspensions by virtue of the fact that PAA is a kind of anionic polyelectrolyte, hydrolyzing a little even not at all in the range of pH < 2.0; while pH > 2.0 the negatively charged organic groups of dissociated PAA molecular prone to adsorbing onto positively charged 8YSZ particle surface results in neutralizing the surface charges of YSZ particles and hence IEP is removed

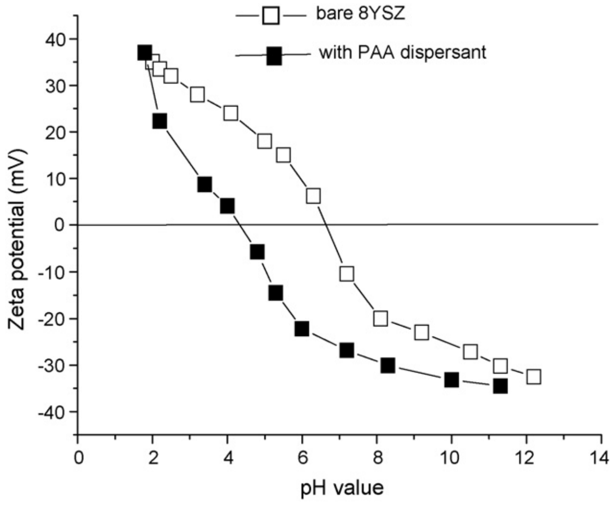

Fig. 1. 8YSZ particle surface Zeta potential as a function of pH value with and without dispersant PAA.

toward acidic region. The formula (2) represents the mechanism of PAA dissociation equilibrium in aqueous solution under various pH conditions:

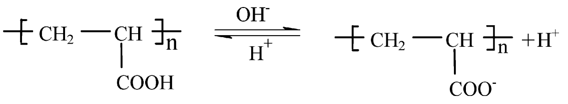

$$\left[CH_2 - \underset{\displaystyle COOH}{CH} \right]_n \underset{H^+}{\overset{OH^-}{\rightleftharpoons}} \left[CH_2 - \underset{\displaystyle COO^-}{CH} \right]_n + H^+ \qquad (2)$$

3.2. Preparation and dispersion mechanism of 8YSZ suspensions

3.2.1. Effect of pH value on YSZ suspensions rheology

Fig. 2 shows the relationship of 8YSZ suspensions apparent viscosity versus pH value. Sample suspensions were composed of 10 vol.% solid content and the 23.0 wt.% concentration of the dispersant PAA expressed relatively to the dry powder weight (dwb.%). As seen from Fig. 2, the apparent viscosity reaches one maximum value (pH 4.6) and two platform regions (in range of pH < 2.4 and pH > 9.0). In strongly acidic region pH < 2.4, according to the formula (2), the polymer PAA nearly can not dissociate and play the role of the steric stabilization that prevent YSZ particles from inter-attracting, moreover, the positively charges YSZ particles repulse from each other, thus, which lead to the suspensions having a lower viscosity and easily flowing. As lowing acidic degree up to pH 4.2 (the IEP of YSZ), non-adsorbed PAA in suspensions have dissociated partly, their stretched molecular long chains tend to tangle as well as the interplays of hydrogen bonds between in molecules, which induces a viscosity increase and aggravates the coalescences and flocculation of particles. When the acidic degree was decreased, PAA molecules tended to dissociate completely and the synergetic effects of the electrostatic and steric repulsion between particles became obvious, thus, the viscosity of suspensions dropped, which help for particles migrating on. While at pH > 10, the system ζ potential was measured as mean −35mV possibly because the adsorbed PAA molecular in suspensions got fully unfolding, which reduced weak inner friction and in favor of free flowing between particles, so the suspensions viscosity reaches the least value. Jing et al. [13] confirm that the phenomenon of keeping ζ potential constant in larger pH region results from the very strong buffering capacity of polyacrilic ammonium. It is worth noting that the interacting mechanisms between the doped-Y_2O_3 dissolved in acid solution in addition to the hydrogen bond and the YSZ colloidal particles need more researches [8–10,12]. Fig. 2 simultaneously indicates that the rheologic character of 8YSZ suspensions was of a non-Newtonian type possessing apparent thixotropic behaviors with the increasing shearing rate.

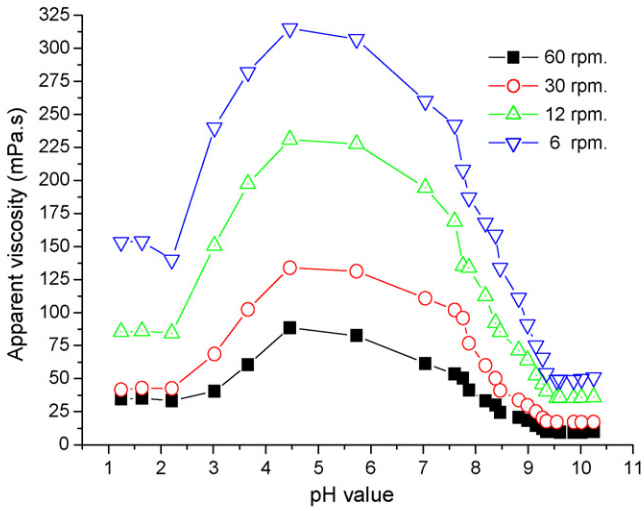

Fig. 2. 8YSZ suspensions apparent viscosity vs. pH value.

3.2.2. Interactions between PAA and YSZ

Water-soluble PAA with low molecular weight (Mw < 5000 Da) as dispersant can modify the surface properties of ceramic particles, which requires polymer PAA with an appropriate molecular weight considering to the unfavorable impacts of the excessive long chains segments of the organic polymer on the dispersion of the ceramic powder. Santhiya et al. [14] found that the adsorption density of PAA in the system composed of PAA and Al_2O_3–H_2O increased as the molecular weight of PAA increasing due to the higher molecular weight PAA with stronger adsorbed free energy. In other words, the interactions between PAA and solid particle surfaces became stronger. In this sense, the suspensions tended to flocculation and lead to agglomeration using PAA with high molecular weight as dispersant. Fig. 3 illustrates the morphologies of 8YSZ suspensions dispersed by 3.0 wt.% (dwb.%) PAA with two kinds of molecular weight at pH 10.07. The dispersion in Fig. 3(a) is better than that of Fig. 3(b) showing more YSZ agglomerates, which coincides with the facts that the 8YSZ agglomerations of Fig. 3(a) used a PAA with molecular weight 5000 as dispersant are more easy to be destroyed under proper ball-milled or ultrasonically dispersed conditions than that with 50,000 PAA used in Fig. 3(b).

The dispersant PAA saturate adsorption volume in suspensions is recognized as the optimum dosage, which is a key parameter in preparation of the desired YSZ suspensions. Fig. 4 demonstrates the differential thermal and the thermal gravity curves of 8YSZ suspensions with solid content 13 wt.% at pH 10.04. Both the (a) and (b) samples were prepared by the same procedure, the YSZ sample was mixed with 3.0 wt.% (dwb.%) PAA (Mw = 5000) and ball-milled till to reach completely adsorbed saturation after 24 h, then the particles and the supernatant were separated by centrifugation, followed by washing several times using de-ionized water and finally dried in oven at a certain temperature. Only another 20.0 wt.% (dwb.%) PAA (Mw = 20,000) for (b) were added into the suspensions to adjust the viscosity approving to dip-coating process. The experiments reported by Wang and Gao [15] are close to our works, it was believed that the optimum dispersant dosage should not surpass 2.0 dwb.% avoiding the presence of unexpected high viscosity and yield value or even weak flocculation. Fig. 4 (a) and (b) differential thermal curves show two exothermal peaks in the range 298–426 °C and 866–1100 °C; correspondingly there are two 1.65% (Fig. 4a) and 5.70% (Fig. 4b) mass loss individually in thermal gravity curves from 298 °C to 426 °C owing to the combustion of PAA

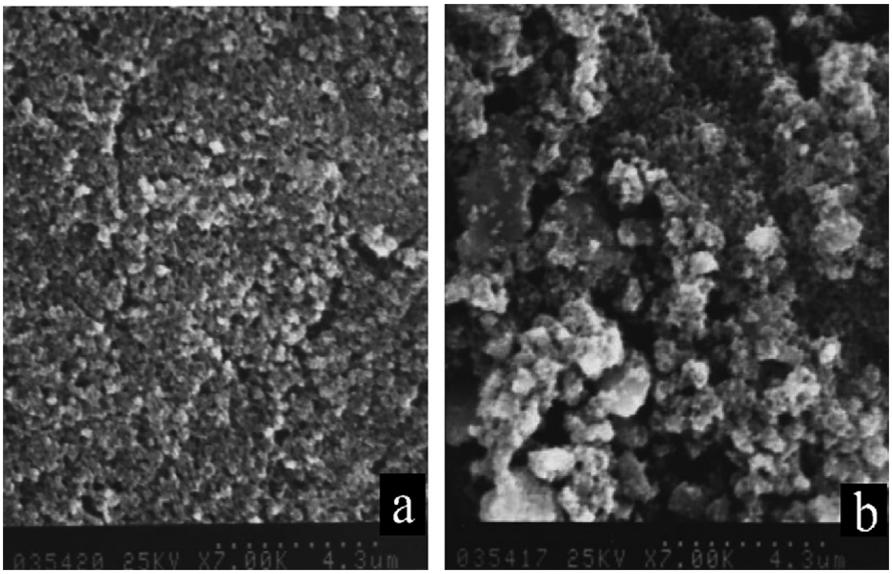

Fig. 3. YSZ particle morphologies of dispersion with different molecular weight PAA-NH4: (a) with PAA 5000 Da.; (b) with PAA 50,000 Da.

adsorbed onto the YSZ particles. Moreover, the complicated combination reactions of oxide impurities maybe give rise to exothermal effects in 866–1100 °C. The FT-IR spectra of the suspensions respectively corresponding to Fig. 4 (a) and (b) are presented in Fig. 5(a) and (b). The distinctive IR spectrum peak of cubic ZrO_2 at 416 cm^{-1} corresponds to the peak at 472 cm^{-1} (a) and 464 cm^{-1} (b) in Fig. 5 respectively on account of the interactions of YSZ and PAA; the peaks of 3422 cm^{-1}, 3424 cm^{-1} represent for that of –OH group; the 2339 cm^{-1} for –CH distinctive peak; 1647–1714 cm^{-1} for –C═O characteristic adsorption peak; 1636 cm^{-1} for C═C; 1402 cm^{-1}, 1422–1562 cm^{-1} for the asymmetric, symmetric flexing and vibrating motions of –COO group; 1068 cm^{-1} for $–CH_2$ distinctive peak [16]. Table 1 indicates an increasing contents of PAA (Mw = 5000) favors for the suspensions stability in the range of pH 10.03–10.20. According to the results reported by Wang and Gao [15] and the data of Fig. 4(a), it was concluded that the viscosity dropped drastically as the dispersant dosage increased so long as not surpassing the saturate adsorption volume, hence the dispersion and the stability elevated corresponding to the lower sedimentation value listed in Table 1; simultaneously the

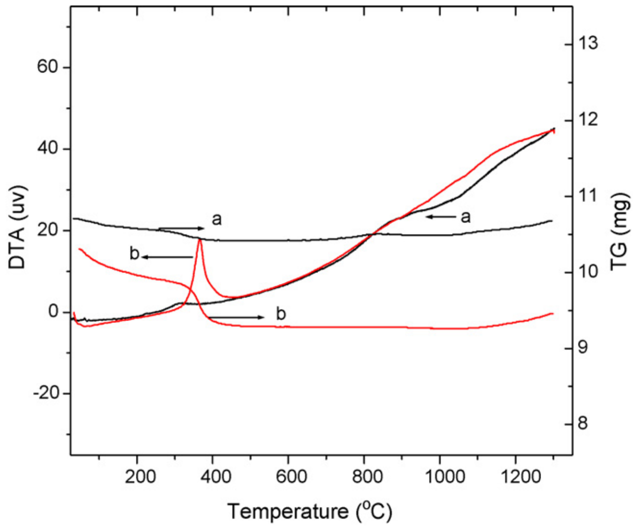

Fig. 4. DTA-TG of 8YSZ suspensions with solid content 13 wt.% and pH 10.04: (a) with PAA 5000 Da; (b) with PAA 50,000 Da and PAA 20,000 Da simultaneously.

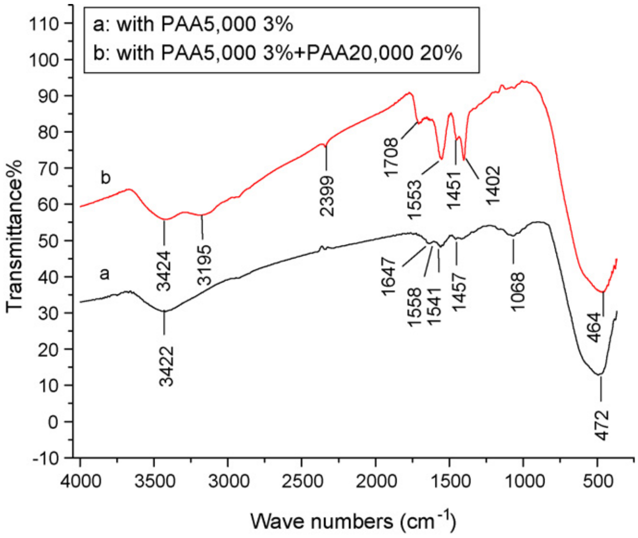

Fig. 5. FT-IR spectra of the interaction between PAA and 8YSZ.

Table 1
Effect of PAA content on the stability of 8YSZ suspensions

Number	PAA content (wt.%)	Solid loading (wt.%)	Sediment value (%)	pH value (18 °C)
1	0.3	23.4	13.3	10.04
2	0.5	23.4	11.6	10.20
3	0.7	23.4	10.8	10.03
4	1.0	23.4	7.5	10.12

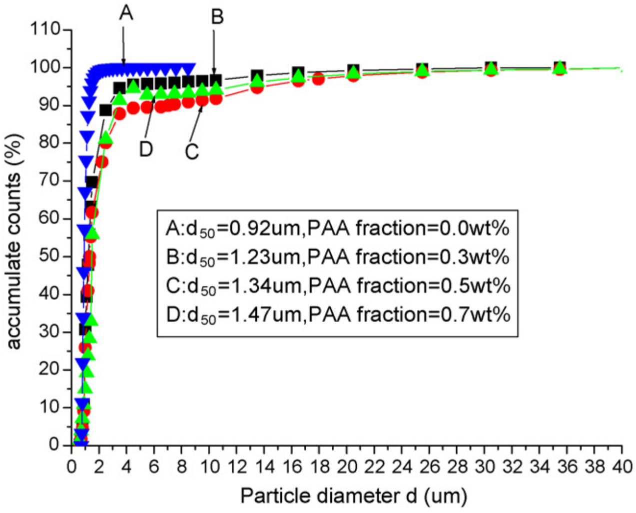

Fig. 6. Effect of PAA content on the particle size of 8YSZ suspensions.

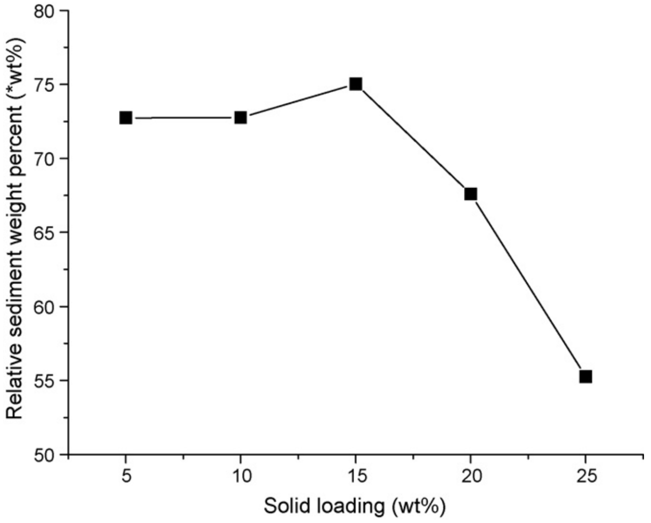

Fig. 7. Effect of solid loading of suspensions on apparent stability.

interactions of YSZ particles and PAA belongs to low affinity adsorption in basic solution and the organic group sides of partly dissociated PAA adsorbed onto the particle surface begin to stretch from initial winding making the YSZ particles size bigger. The increasing particle size from $d_{50} = 0.92$ μm to 1.47 μm is illustrated in Fig. 6. Liu [17] thought that this was due to the unsaturated coated YSZ particles having necklaces-like soft agglomeration structures bridged or tangled by the polymer and could be avoided by increasing the dispersant fraction till reaching saturate adsorption.

In a summary, according to the results mentioned above, it is concluded that the dispersing and stabilizing mechanism of YSZ suspensions perhaps can be described. The positively charged solid particle surface are firstly saturated by adsorption of negatively charged PAA through hydrogen bonds or other chemical bonds in basic circumstances, which result in the increasing effective thickness of colloidal particle electric double layer and elevate the ζ potential of the suspensions. The electrostatic repulsions derived from the DLVO theory and the adsorbing polymer steric roles prevent the YSZ powder from agglomerating. The exceeding, non-adsorbing free PAA existing in colloidal YSZ interparticle gaps also can improve the stability of dispersed particles due to the depletant effects and hence adjust the suspensions viscosity more or less [18].

3.2.3. Influence of solid loading

The solid loading influences not only the ceramic membrane thickness but also the suspensions stability. Fig. 7 shows the relationship between solid content and suspensions stability with PAA addition 3.0 dwb.% at pH 10.03. As seen from the graph, the sedimentation value firstly were almost impregnable to the solid content varying from 5.0 wt.% to 10.0 wt.% then increased to the maximum value with the solid loading 10–15 wt.%. However, the apparent stability was improved as the increasing solid loading from 15 wt.% to 25 wt.%. According to the Woodcock formula Eq. (3) and the Que mada model Eq. (4) [19]:

$$\frac{h}{d} = \left(\frac{1}{3\pi\phi} + \frac{5}{6}\right)^{1/2} - 1 \qquad (3)$$

$$\eta_r = \left(1 - \frac{\phi}{\phi_m}\right)^{-2} \qquad (4)$$

where, h is the average distances between the closest two suspending particles, d the particle size, ϕ the volume fraction of solid, ϕ_m the maximum packing fraction of solid particle and its value relates to the particle shape in the range of 0.5–0.75, η_r is the relative viscosity of the suspension with respect to the suspending fluid at a given shear rate. The above formulas indicate that the h reduces and the η_r arises as the solid content (ϕ) elevates under the given ϕ_m value and the known d value. Therefore, the friction originating from the proximate colloidal particles and the electrostatic repulsions will increase preventing the separated ceramic particles from agglomerating for the spectrum of solid loading (15 wt.% $< \phi <$ 25 wt.%) while the interactions of colloidal particle are obscure due to the further separation between dispersed ceramic particles over the solid loading range $\phi <$ 10 wt.%, but the probability of collisions with colloidal particles each other enhances as the solid loading increases from 10 wt.% to 15 wt.%.

3.2.4. Effect of the temperature

Fig. 8 shows the dependences of the rheology of YSZ suspensions dispersed with PAA 3.0 dwb.% on the temperature with the solid loading 16.30 wt.% at pH 10.03. Based on the results shown in Fig. 8, the suspensions apparent viscosity drops from 31.06 mPa s to 10.4 mPa s at a rotate rate of 60 rpm as the temperature increases in the range 18.5–45.0 °C, which are similar to the results of the aqueous titanium dioxide dispersions reported by Miculášek and Wakeman [20] but opposite against those findings of Guo and Zhang [21] with aqueous alumina slurry. In addition, Fig. 8 also reveals the

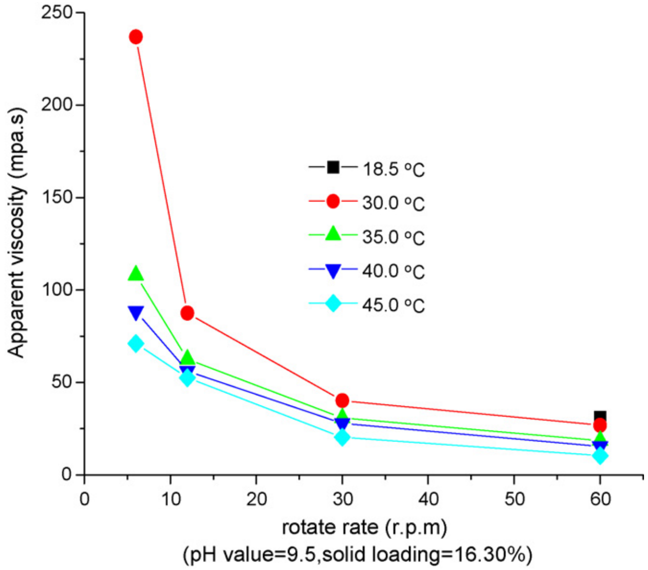

Fig. 8. Effect of temperature on the 8YSZ suspensions rheology.

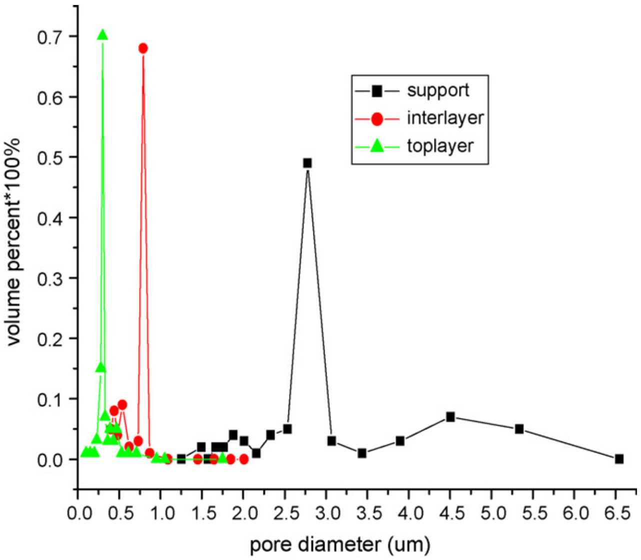

Fig. 10. Pore diameter and distribution of 8YSZ/Al_2O_3 membrane.

suspensions obvious shear-thinning behavior along with the little effects of temperature on the apparent viscosity in the higher shear rate region. Although the mechanisms of the dependences of the YSZ suspensions rheology on the temperature variations yet remain ambiguous up to now, it was believed by Miculášek and Wakeman [20] that the location of shear-thinning region was dependent upon the relative strength of Brownian and the shear-induced flow contributions, i.e., the Brownian motions of particles are dominate over the shear-induced motions (hydrodynamic effects) contribution to the particles interactions in the low shear rate region whereas in the high shear rate region, the shear-induced motions are expected to be in control. However, Guo and Zhang [21] thought that the adsorption of dispersant increased with the increasing temperature and the stability of slurry was strongly dependent on the adsorption state of dispersant. Hence, the dispersant became insufficient as temperature increased in low dispersant concentration resulting in the increasing viscosity. As stated, the amounts of PAA 3.0 wt.% is sufficiently enough to reach a complete surface coverage for YSZ particles, thus, it is presented in Fig. 8 that the apparent viscosity drops as the increasing temperature.

3.3. 8YSZ ceramic membrane performances

Fig. 9 show the SEM morphology of 8YSZ microfiltration membranes made from the 8YSZ suspensions described above subsequently by dip-coating, drying, sintering at 1350 °C for 2 h. The membrane surface with pore size about 0.30 μm (Fig. 9a) is smooth, crack-free and the fracture photograph (Fig. 9b) indicates the membrane thickness is about 10.0 μm with a close connection between the interlayer and the top layer. Fig. 10 illustrates the pore size and its distribution of 8YSZ membrane. As seen from Fig. 10, the median pore size 0.31 μm and the maximum pore size 0.71 μm were obtained, the

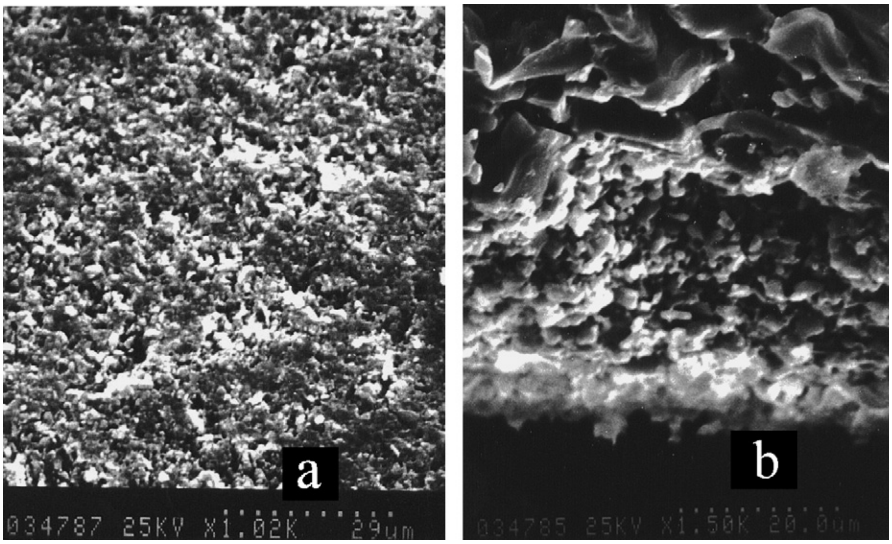

Fig. 9. 8YSZ microfiltration membran microstructure: (a) membrane surface; (b) membrane cross-section

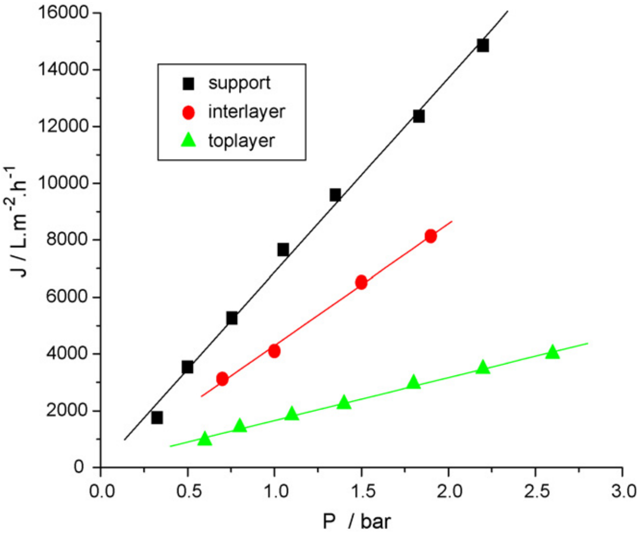

Fig. 11. Linear fitted clean water flux of 8YSZ/Al_2O_3 membrane.

distribution of pore size is narrower than that of the support and the interlayer, which in turn implies the pore structures created by the well dispersed 8YSZ particles are quite reasonable. Fig. 11 demonstrates the relationship of the pure water flux with the transmembrane pressure at 20 °C. The desired pure water permeability1.7 $m^3 h^{-1} bar^{-1} m^{-2}$ shown by Fig. 11 was got, which attained to that 0.4–1.5 $m^3 h^{-1} bar^{-1} m^{-2}$ of the ZrO_2/Al_2O_3 composite membrane reported by Chao et al. [8]. Indeed, somewhat performance discrepancies like pore size and chemical stability between prepared membranes and the reported one are still existed, which were perhaps caused by the factors such as the selected membranes materials and the specific support quality.

4. Conclusions

1. The commercial available 8YSZ powder was successfully utilized to prepare stable suspensions required for dip-coating membranes on porous support. It is confirmed that through selecting appropriate dispersing conditions, the uniform and stabilized 8YSZ suspensions with appropriate viscosity could be realized very easy.
2. In 8YSZ–H_2O–PAA–NH_4 ternary system, the stability of the suspensions is apparently dependent on the dissociated degree of the PAA under different pH value, which is determined from the balance between the Vander Walls attraction and the electrosteric repulsion of the dissociated polyelectrolyte as well as depletants effects of free PAA in solution. The improving dispersion requires both dispersant having appropriate molecular weight, saturation adsorption onto the YSZ particles and the suspensions with desired solid content and a given temperature.
3. The membrane performances from the 8YSZ suspensions were characterized in terms of membrane thickness of 10 μm or so, pure water permeability 1.7 $m^3 h^{-1} bar^{-1} m^{-2}$ and the median pore diameter 0.31 μm. The SEM images of membrane microstructure demonstrate that top-layer membranes close bonding to support have no defects, which is expected to be further serviced as high quality supports for ultra-thin dense YSZ and other ceramic or metallic membranes in various application fields.

Acknowledgements

This work was supported by the Natural Science Foundation of China under contract No. 20271047 and the Ministry of Science and Technology of China under contract No. 2003CB615700 and 2001AA323090.

References

[1] J. Zaman, A. Chakma, Inorganic membrane reactors, J. Membr. Sci. 92 (1994) 1–28.
[2] R. Gopalan, C.H. Chang, Y.S. Lin, Thermal stability improvement on pore and phase structure of sol–gel derived zirconia, J. Mater. Sci. 30 (1995) 3075–3081.
[3] X. Changrong, et al., Preparation of yttria stabilized zirconia membranes on porous substrates by a dip-coating process, Solid State Ionics 133 (2000) 287–294.
[4] J. Kim, Y.S. Lin, Sol–gel synthesis and characterization of yttria stabilized zirconia membranes, J. Membr. Sci. 139 (1998) 75–83.
[5] X. Ju, P. Huang, N. Xu, J. Shi, Influence of sol and phase stability on the structure and performance of mesoporous zirconia membrane, J. Membr. Sci. 166 (2000) 41–50.
[6] J. Kim, Y.S. Lin, Synthesis and characterization of suspension-derived, porous ion-conducting ceramic membranes, J. Am. Ceram. Soc. 82 (10) (1999) 2641–2646.
[7] Y. Zhang, J. Gao, et al., Dip-coating thin yttria-stabilized zirconia films for solid oxide fuel cell applications, Ceram. Int. 30 (2004) 1049–1053.
[8] Y. Chao, et al., Preparation and application in oil–water separation of ZrO_2/Al_2O_3 MF membrane, J. Membr. Sci. 142 (1998) 235–243.
[9] R. Greenwood, K. Kendall, Acoustophoretic studies of aqueous suspensions of alumina and 8.0 mol.% yttria stabilised zirconia powders, J. Eur. Ceram. Soc. 20 (2000) 77–84.
[10] J.J. Swab, low temperature degradation of Y–TZP materials, J. Mater. Sci. 26 (1991) 6706–6714.
[11] T. Fengqiu, et al., Effect of dispersants on surface chemical properties of nano-zirconia suspensions, Ceram. Int. 26 (2000) 93–97.
[12] F. Shojai, et al., Electrostatic and electrosteric stabilization of aqueous slip of 3Y–ZrO_2 powder, J. Eur. Ceram. Soc. 20 (2000) 277–283.
[13] S. Jing, et al., Quantitatively adsorption of polyacrlic ammonium onto nanometer Y-TZP powder, J. Inorg. Mater. (in chinese) 14 (4) (1998) 645–649.
[14] D. Santhiya, et al., Effect of polymer molecular weight on the adsorption of polyacrlic acid at the alumina-water interface, Colloid Surf. A: Physicochem. Eng. Aspects 133 (1998) 157–163.
[15] J. Wang, L. Gao, Surface and electrokinetic properties of Y-TZP suspensions stabilized by polyelectrolytes, Ceram. Int. 26 (2000) 187–191.
[16] G.Y. Guo, Y.L. Chen, Preparation and characterization of a novel zirconia precursor, Ceram. Int. 30 (2004) 469–475.
[17] D.-M. Liu, Influence of dispersant on powders dispersion and properties of zirconia green compacts, Ceram. Int. 26 (2000) 279–287.
[18] J.A. Lewis, Colloidal processing of ceramics, J. Am. Ceram. Soc. 83 (10) (2000) 2341–2359.
[19] H.A. Barnes, J.H. Hutton, K. Walters, An Introduction to Rheology. Rheology Ser. 3, Elsevier, Amsterdan, 1989.
[20] P. Miculášsk, R.J. Wakeman, et al., The influence of pH and temperature on the rheology and stability of aqueous titanium dioxide dispersions, Chem. Eng. J. 67 (1997) 97–102.
[21] L.-C. Guo, Y. Zhang, et al., Influence of temperature on stability of aqueous alumina slurry containing polyelectrolyte dispersant, J. Eur. Ceram. Soc. 17 (1997) 345–350.